Locally enhanced precipitation organized by planetary-scale waves on Titan

Jonathan L. Mitchell,[1*] Máté Ádámkovics,[2] Rodrigo Caballero,[3,4] Elizabeth P. Turtle[5]

[1]Earth & Space Sciences, Atmospheric & Oceanic Sciences
University of California, Los Angeles, CA 90095, USA
[2]Astronomy Department, University of California, Berkeley, CA 94720, USA
[3]Department of Meteorology (MISU), Stockholm University, Stockholm, Sweden
[4]Bert Bolin Centre for Climate Research, Stockholm University, Stockholm, Sweden
[5]Johns Hopkins University, Applied Physics Laboratory, Laurel, MD 20723, USA

June 24, 2011

Abstract

Titan exhibits an active weather cycle involving methane[1, 2, 3, 4, 5, 6, 7, 8]. Equatorial and midlatitude clouds recently observed by NASA's Cassini spacecraft appear organized into fascinating morphologies on scales exceeding 1000 km[9], including an arrow-shaped equatorial cloud which produced detectable surface accumulation, presumably from liquid methane precipitation[10]. Analysis of an earlier cloud outburst also indicated an interplay between high- and low-latitude cloud activity mediated by planetary-scale atmospheric waves[11]. Here we provide a general physical interpretation of observed storms, their relation to atmospheric dynamics and their aggregate effect on surface erosion through a combined analysis of cloud observations and simulations, opening a new field of dynamic meteorology on Titan. We demonstrate that planetary-scale Kelvin waves naturally arising in a new, three-dimensional version of our Titan general circulation model (GCM) robustly organize convection into chevron-shaped storms at the equator during the equinoctial season. A second and much slower wave mode organizes convection into southern-hemisphere streaks oriented northwest-southeast, similar to another recently observed cloud[9]. The phasing of these modes causes a 20-fold increase in precipitation rates over the average, each event producing up to several centimeters of precipitation over 1000-km-scale regions, with important implications for observed fluvial features[12].

Titan's slow rotation (16 terrestrial days) and small radius (40% that of Earth) conspire to allow a global Hadley circulation, the tropical meridional overturning circulation of the atmosphere. As a result, Titan's strongest zonal winds are shifted poleward relative to Earth's, meridional temperature gradients are weak[13], and baroclinic cyclogenesis associated with storm-track weather is suppressed[14]. This dynamical configuration gives Titan an "all tropics" climate[15]. Titan's Inter-tropical Convergence Zone (ITCZ) migrates from one summer hemisphere to the other. Models predict a transient phase just following equinoxes when the ITCZ passes over the equator[15, 16, 17], and during this time, Earth-like tropical disturbances would be expected at Titan's equator[18, 9].

1

Classical shallow-water theory[19] predicts the existence of a broad spectrum of linear equatorial wave modes, including equatorially-trapped Rossby, Kelvin and mixed Rossby-gravity waves. All of these modes can be detected in Earth's atmosphere through spectral analysis of observations, which show power concentrated at planetary scales ($> 10^4$ km)[20]. Through their surface convergence and induced vertical motion, the modes collectively organize the location and timing of clouds and precipitation in Earth's tropics on intraseasonal timescales. Because of low insolation and a stabilizing antigreenhouse effect[21], moist convection on Titan cannot be maintained purely through surface evaporative fluxes, indicating that moisture convergence provided by large-scale modes of circulation is important for convective cloud formation[15, 18, 17, 22, 23].

Titan's methane clouds have received much attention since they were first discovered spectroscopically[1]. Although cloud-cover is spatially limited, dramatic outbursts of cloud activity occasionally occur[24] as do cloud-free conditions[25]. Mesoscale clouds can remain stationary for days[23, 26, 27]. Titan's seasons progress slowly, taking roughly seven years to transition from solstice to equinox. The most recent northern spring equinox (NSE) occurred on 11 August 2009. Since that time, the location of cloud activity has shifted from southern (summer) mid and high latitudes to the equatorial region[27, 28, 9].

More recently, Cassini Imaging Science Subsystem (ISS) images of Titan have revealed large-scale clouds with an interesting array of morphologies and characteristics[9]. Most strikingly, an arrow-shaped cloud oriented eastward was observed at the equator on 27 September 2010[9], followed by observations of surface wetting which gradually diminished over several months[10]. We now use our fully three-dimensional Titan GCM (described in Methods and SI) to illuminate the dynamical origin of these storms, and we develop a methodology for comparing model precipitation rates to cloud observations.

Cloud opacity depends on the sizes and amount of suspended, condensed methane. Our Titan GCM has a moist convection scheme which predicts a surface precipitation rate, and we assume precipitation is associated with optically thick clouds. A small number of physically motivated assumptions (described in Methods and SI) allow us to simulate cloud opacity in ISS bands using the GCM's precipitation field, thereby quantitatively linking cloud opacity to the amount of precipitation. Simulated observations of two events during the equinoctial transition of our GCM are displayed in Figs. 1b and 1e. The two cloud events observed by Cassini ISS are shown in Figs. 1c and 1f: a cloud shaped like a chevron at the equator pointing eastward was observed on 27 September 2010, followed on 18 October 2010 by a streak of clouds extending southeastward from low-latitudes to high-latitudes[9]. Fig. 1 demonstrates that our Titan GCM produces convective storms with the basic morphology of the two cloud observations. The dynamics underlying these storms are now illustrated through diagnostics of the GCM.

Fig. 2 shows snapshots of the GCM simulation of Titan shortly following NSE. During this time, the ITCZ is passing over the equator and establishing itself in the northern hemisphere (Fig. S7). Figs. 2a and 2c show the surface wind field with the zonal mean subtracted (arrows) and the 15-day cumulative precipitation of the events shown in Figs. 1b and 1e (blue, cm). The cumulative precipitation of these storms indicates greatly enhanced precipitation rates compared to the global- and time-mean of less than 0.1 mm/day. Near the equator, zonally elongated bands of precipitation are being maintained by the circulation, marking the location of the ITCZ. Fig. 2a clearly shows a chevron precipitation feature at 100° longitude at the equator that is spatially coincident with a region of horizontal convergence of surface winds, indicating a role for gravity waves. The chevron produces one to two centimeters of precipitation over a 2000-km-wide region during its lifetime, an amount sufficient to create runoff and erosion of the equatorial surface[29]. A few months of

2

integration later, the model produces a precipitation and wind pattern extending from the equator deep into the southern hemisphere as seen in Fig. 2c. This streaking precipitation is produced by a combination of convergent and circulating surface winds, indicating a role for both gravity waves and Rossby waves. The depth of convection in the streaking feature is shallower than the chevron (Fig. S6), however its lifetime is considerably longer resulting in several centimeters of precipitation over its extent. Currently published ISS images do not show evidence for surface changes associated with the storm in Fig. 1f, which suggests these clouds do not produce substantial rainfall. This indicates that our model overestimates the amount of midlatitude precipitation during the current season.

Precipitation rates within these modes exceed the zonal- and time-mean rate by a factor of $\sim$20 during the equinoctial transition (Fig. 3a). We infer that three-dimensional dynamics is responsible for local and significant enhancements in precipitation, and therefore essential for understanding the observed distribution of surface erosion[12]. Equatorial chevrons are ephemeral features of Titan's climate, however, occurring of order an Earth year as Titan's ITCZ undergoes a post-equinoctial transition from one hemisphere to the other (Figs. S7 and S10)[18]. Surface accumulation (that does not infiltrate into the regolith) evaporates away during the summer (Fig. S8), with important implications for observed fluvial features in Titan's semi-arid environment[12].

We now show that the cloud structures in the examples above are not isolated occurrences, but instead constitute the 'typical' behavior of convection in the model, organized by well-defined dynamical modes of the atmosphere. The evolution in time and longitude of modeled equatorial precipitation (Fig. 3a) shows evidence of eastward-propagating disturbances with a phase speed of about 12 m s^{-1} (indicated by the solid black line), superposed on slower disturbances traveling westward at around 1 m s^{-1} (dashed line). These two modes of variability are also apparent in a space-time power spectrum of equatorial surface zonal wind (Fig. 3b), which shows sharp peaks at eastward-propagating zonal wavenumber 2 with a period of about 8 days (corresponding to a phase speed of about 12 m s^{-1} at the equator) and at westward-propagating zonal wavenumber 2 with period $\sim$ 100 days (phase speed $\sim$ 1 m s^{-1}). This close correspondence between precipitation and surface wind perturbations implies a link between dynamical and convective processes, as seen in convectively-coupled equatorial waves on Earth [20].

To isolate the spatial structure of the dominant eastward and westward modes, we follow a three-step procedure described in the Methods section. The spatial structure and phase speed of the eastward-propagating mode corresponds closely to that of a baroclinic, equatorially-trapped Kelvin wave (see SI). The spatial patterns of precipitation and surface wind anomaly of this mode are shown in Fig. 2c. Crucially, these waves are associated with roughly chevron-shaped equatorial precipitation patterns. The westward-propagating mode (Fig. 2d) stretches from the equator to the high latitudes of the Southern Hemisphere, and is associated with a streak-like precipitation feature stretching southeastwards from the tropics into the midlatitudes. Thus, convective storms in the GCM are organized by large-scale modes of variability, and the modes are robustly associated in a statistical sense with precipitation structures resembling observed clouds.

We have also conducted sensitivity tests to investigate the feedback of moist convective heating onto the dynamical modes (see SI for details). In a simulation where latent heating by convection and surface evaporation is artificially suppressed, we find that the eastward-propagating Kelvin mode is unchanged, while the westward mode is substantially altered (Fig. 3c). Thus the Kelvin mode is convectively uncoupled (see SI), though its surface convergence field plays an important role in organizing precipitation. Convection is essential to the dynamics of the westward mode, however, as indicated by the substantial reduction of precipitation at negative wavenumbers in

the test case (Fig. 3c; also see SI). This is the first evidence of a convectively-coupled wave on a planetary body other than Earth.

A sequence of cloud observations taken in 2008 (before NSE) with ground-based instruments indicated a connection between disturbances at equatorial and polar latitudes likely to be mediated by planetary-scale waves [11]. This cloud propagated eastward at $\sim$3 m/s, and was interpreted as a stationary Rossby wave advected by the mid-tropospheric wind. However, our simulation indicates the eastward-propagating precipitation field during this epoch is associated with the Kelvin wave component. Since this observation occurred before NSE, surface convergence resulting from the superposition of the Kelvin mode and the ITCZ is most intense south of the equator (Fig. S10). As the season transitions towards Northern Summer Solstice (NSS), our model indicates a shift in the precipitation by the Kelvin-ITCZ superposition to northern mid latitudes accompanied by southern mid-latitude streaks. We therefore predict a phase of transient cloud activity in both hemispheres of Titan during the next several years (Fig. S7).

In summary, we have developed a process for interpreting morphologies of and precipitation associated with Titan's clouds through a combined analysis of observations and GCM simulations, thereby opening a new field of dynamic meteorology. We find that recent cloud activity near Titan's equator just following NSE is consistent with the presence of two dominant modes of atmospheric variability in the GCM. A fast, eastward-propagating mode traveling at $\sim$12 m s^{-1} with the character of an equatorially-trapped Kelvin wave produces chevron-shaped precipitation patterns similar to the clouds observed by Cassini ISS on 27 September 2010[9]. A slow, westward-propagating mode that is vertically confined accounts for streaks of precipitation like the cloud observed on 18 October 2010[9]. This latter mode is convectively coupled, the first of its kind to be inferred outside of Earth's atmosphere. The phasing of these modes produce several centimeters of precipitation over 1000-km-scale regions, locally enhancing precipitation rates by 20-fold over the mean. These modes therefore play a crucial role in fluvial erosion of Titan's surface. Observations clearly indicate surface changes associated with the equatorial chevron[10], but precipitation from the midlatitude streak is too light to be detected, indicating the model overestimates mid-latitude precipitation during the current season.

Methods

Our Titan GCM is similar to that used in a previous study[17], the primary difference being that the model is now fully three-dimensional. Simplified treatments of radiation, convection, and the seasonal cycle are included. The model does not include tides, either thermal (diurnal) or gravitational (semi-diurnal), nor any other non-axisymmetric forcing mechanism (be it topography, albedo, opacity sources, etc.). The atmosphere is spun up and moistened by methane evaporation from an initial state of solid-body rotation and zero methane humidity. The seasonal cycle of insolation is included in the model forcing; see the SI for a more detailed description. A (statistical) steady-state is achieved after $\sim$20 Titan years ($\sim$600 Earth years). The results shown in figures are from 1000 terrestrial days bracketing NSE of the 21st simulated Titan year. (The zonal- and time-mean overturning streamfunction, zonal winds, and temperature of the full, 1800 model days are shown in the SI.)

The GCM does not include a cloud scheme, so we have developed a method for simulating cloud observations based on precipitation. Briefly, we assume cloud droplets are distributed about a peak size of 512 μm, which are marginally lofted for convective updrafts of 10 m s^{-1}, typical for deep convective events on Titan[22]. We assume 10 - 20% of the column precipitation remains suspended with a cloud-top altitude of 20 km. Together the column mass of the cloud and the droplet size distribution determine the cloud optical depth. Mie theory then translates the droplet

size distribution into the scattering properties of cloud, ultimately linking the precipitation field from the GCM to the radiative transfer model (see SI for more details).

To isolate the spatial structure of dominant modes of variability in the GCM, the surface zonal wind field is spectrally filtered to retain only the space and time scales of the dominant spectral peaks; the leading patterns of variability of the filtered surface wind are extracted using empirical orthogonal function (EOF) analysis, and the associated three-dimensional fields are reconstructed by regression onto the leading principal component; further details are given in the SI.

References

[1] Griffith, C., Owen, T., Miller, G. & Geballe, T. Transient clouds in Titan's lower atmosphere. *Nature* **395**, 575–578 (1998).

[2] Griffith, C., Hall, J. & Geballe, T. Detection of daily clouds on Titan. *Science* **290**, 509–513 (2000).

[3] Tokano, T. *et al.* Methane drizzle on Titan. *Nature* **442**, 432–435 (2006).

[4] Ádámkovics, M., Wong, M., Laver, C. & de Pater, I. Widespread morning drizzle on Titan. *Science* **318**, 962–965 (2007).

[5] Brown, M., Smith, A., Chen, C. & Ádámkovics, M. Discovery of fog at the south pole of Titan. *Astrophys. J. Lett.* **706**, L110–L113 (2009).

[6] Turtle, E. *et al.* Cassini imaging of Titan's high-latitude lakes, clouds, and south-polar surface changes. *Geophys. Res. Lett.* **36**, L02204 (2009).

[7] Turtle, E., Perry, J., Hayes, A. & McEwen, A. Shoreline Retreat at Titan's Ontario Lacus and Arrakis Planitia from Cassini Imaging Science Subsystem Observations. *Icarus* **212**, 957–959 (2011).

[8] Hayes, A. G. *et al.* Transient surface liquid in Titan's polar regions from Cassini. *Icarus* **211**, 655–671 (2011).

[9] Turtle, E. *et al.* Seasonal changes in Titan's meteorology. *Geophys. Res. Lett.* **38**, L03203 (2011).

[10] Turtle, E. *et al.* Rapid and extensive surface changes near Titan's equator: Evidence of April showers. *Science* **331**, 1414–1417 (2011).

[11] Schaller, E., Roe, H., Schneider, T. & Brown, M. Storms in the tropics of Titan. *Nature* **460**, 873–875 (2009).

[12] Langhans, M. *et al.* Titan's fluvial valleys: Morphology, distribution, and spectral properties. *Planet. Space Sci.* **In press** (2011).

[13] Achterberg, R., Conrath, B., Gierasch, P., Flasar, F. & Nixon, C. Titan's middle-atmospheric temperatures and dynamics observed by the Cassini Composite Infrared Spectrometer. *Icarus* **194**, 263–277 (2008).

[14] Mitchell, J. & Vallis, G. The transition to superrotation in terrestrial atmospheres. *J. Geophys. Res.* **115**, E12008 (2010).

[15] Mitchell, J., Pierrehumbert, R., Frierson, D. & Caballero, R. The dynamics behind Titan's methane clouds. *Proc. Natl. Acad. Sci. USA* **103**, 18421—18426 (2006).

[16] Tokano, T. Impact of seas/lakes on polar meteorology of Titan: Simulation by a coupled GCM-Sea model. *Icarus* **204**, 619–636 (2009).

[17] Mitchell, J., Pierrehumbert, R., Frierson, D. & Caballero, R. The impact of methane thermodynamics on seasonal convection and circulation in a model Titan atmosphere. *Icarus* **203**, 250–264 (2009).

[18] Mitchell, J. The drying of Titan's dunes: Titan's methane hydrology and its impact on atmospheric circulation. *J. Geophys. Res.* **113**, E08015 (2008).

[19] Matsuno, T. Quasi-geostrophic motions in the equatorial area. *J. Meteor. Soc. Japan* **44**, 25–42 (1966).

[20] Wheeler, M. & Kiladis, G. Convectively coupled equatorial waves: Analysis of clouds and temperature in the wavenumber-frequency domain. *J. Atmos. Sci.* **56**, 374–399 (1999).

[21] McKay, C., Pollack, J. & Courtin, R. The greenhouse and antigreenhouse effects on Titan. *Science* **253**, 1118–1121 (1991).

[22] Barth, E. L. & Rafkin, S. C. R. Convective cloud heights as a diagnostic for methane environment on Titan. *Icarus* **206**, 467–484 (2010).

[23] Ádámkovics, M., Barnes, J., Hartung, M. & de Pater, I. Observations of a stationary mid-latitude cloud system on Titan. *Icarus* **208**, 868–877 (2010).

[24] Schaller, E., Brown, M., Roe, H. & Bouchez, A. A large cloud outburst at Titan's south pole. *Icarus* **182**, 224–229 (2006).

[25] Schaller, E., Brown, M., Roe, H., Bouchez, A. & Trujillo, C. Dissipation of Titan's south polar clouds. *Icarus* **184**, 517–523 (2006).

[26] Roe, H., Brown, M., Schaller, E., Bouchez, A. & Trujillo, C. Geographic control of Titan's mid-latitude clouds. *Science* **310**, 477–479 (2005).

[27] Rodriguez, S. *et al.* Global circulation as the main source of cloud activity on Titan. *Nature* **459**, 678–682 (2009).

[28] Brown, M., Roberts, J. & Schaller, E. Clouds on Titan during the Cassini prime mission: A complete analysis of the VIMS data. *Icarus* **205**, 571–580 (2010).

[29] Jaumann, R. *et al.* Fluvial erosion and post-erosional processes on Titan. *Icarus* **197**, 526–538 (2008).
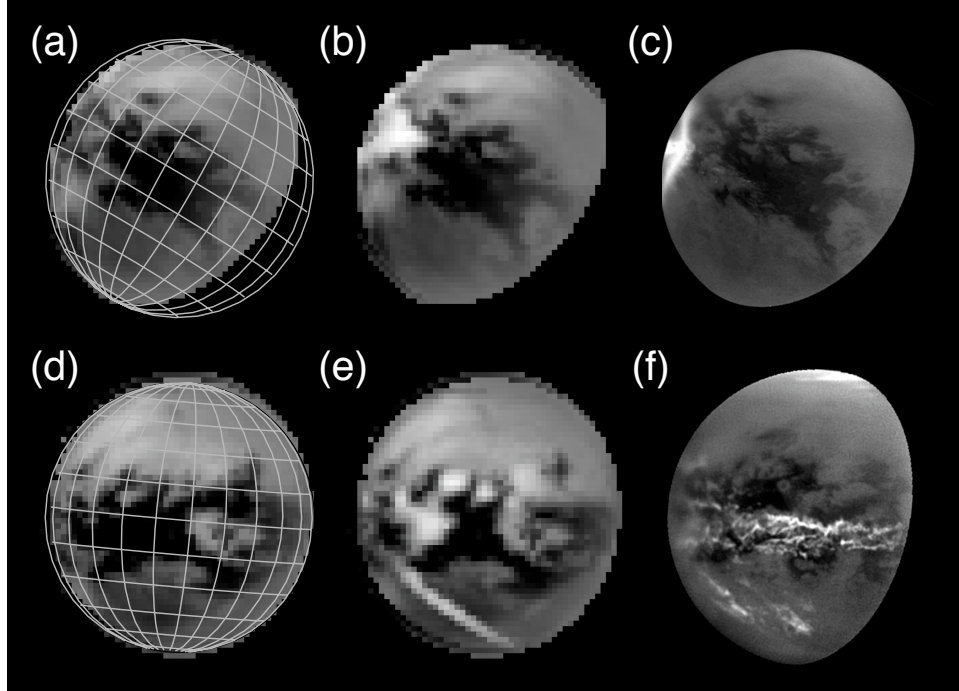
Fig. 1. (a) & (d): Simulations of cloud-free observations at 938nm with lines of latitude and longitude used for comparison with models that include cloud opacity distributions (b) & (e) set by the precipitation from the GCM output as described in Methods (shown in Fig 2). Viewing geometry and illumination angle are selected to reproduce Cassini observations on 27 September 2010 (c) and 18 October 2010 (f)[9]. GCM models (b & e) are divided by a simulated 619nm image to reproduce the image processing used for the observations. No parameter tuning is required to produce a similar contrast to observations, indicating a close correspondence between the modeled precipitation field and the observed clouds.
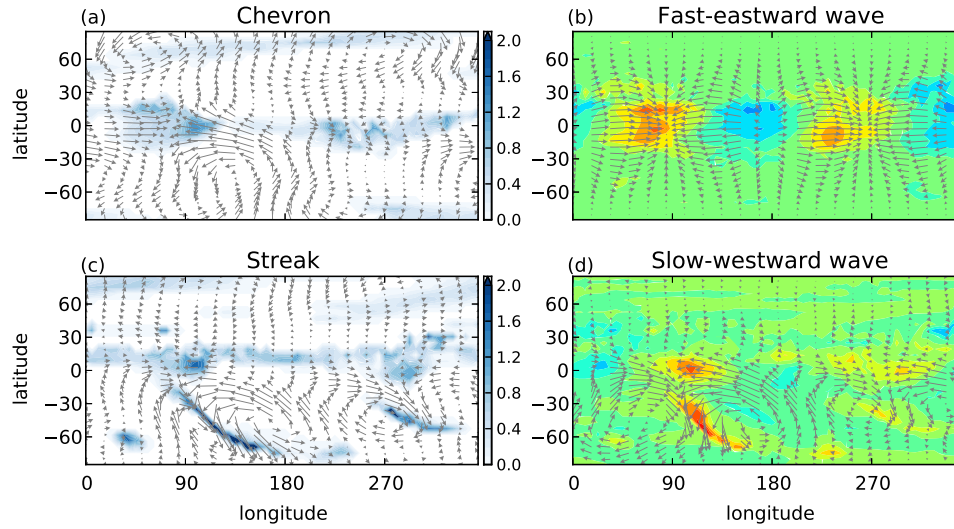
Fig. 2. Simulated precipitation and surface wind patterns in selected events during the equinoctial season (left column) and derived from statistical analysis (right column). (a): Fifteen-terrestrial-day cumulative precipitation (blue, cm) and surface winds with the zonal mean subtracted (arrows) for an equatorial chevron-shaped event. (b): Regression of the leading principal component associated with eastward-propagating variance (see SI) onto the surface winds (arrows) and precipitation (colors). (c): As in (a) but for a midlatitude streak event. The length of wind vector arrows have been increased by a factor of 3. (d): As in (b) but for westward-propagating variance.
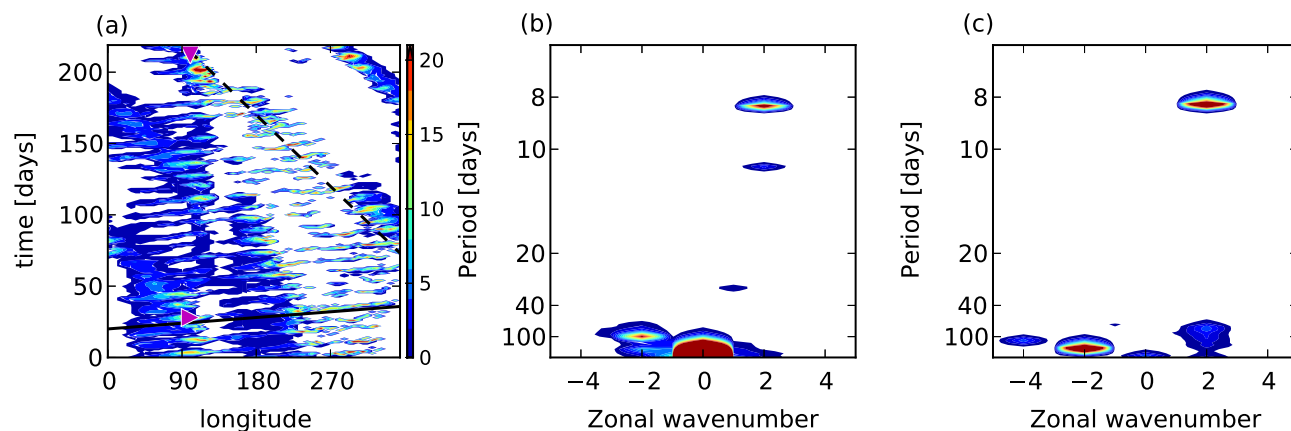
Fig. 3. Space-time variability of simulated equatorial winds and precipitation averaged over $\pm 10°$ latitude in the Titan GCM. (a): Longitude-time distribution of precipitation rate normalized to the global- and time-mean rate for the period containing the chevron event in Fig. 1 (magenta triangle at day 30) and the streak event (triangle at day 210). Lines indicate constant velocity trajectories of 11.7 m s^{-1} eastward (solid) and 0.9 m s^{-1} westward (dashed). (b): Space-time spectral decomposition of surface zonal winds for 1000 simulation days centered around the equinox. (c): As in (b) but for a test simulation with the latent heating of methane removed.